Available online at www.sciencedirect.com
ScienceDirect
Trans. Nonferrous Met. Soc. China 35(2025) 4253−4265
Transactions of Nonferrous Metals Society of China
www.tnmsc.cn

Mechanism, kinetics and process assessment of efficient extraction of valuable metal from nickel sulfide ore by $(NH_4)_2S_2O_8$ direct oxidative leaching

Rui-min YANG[1,2], Wen-ning MU[1,2,3,4], Yuan-hang ZHOU[2,3], Jun-jin MENG[2,3], Xue-fei LEI[2,3,4], Shao-hua LUO[2,3,4], Xue-yong DING[1]

1. School of Metallurgy, Northeastern University, Shenyang 110819, China;
2. School of Resources and Materials, Northeastern University at Qinhuangdao, Qinhuangdao 066004, China;
3. School of Materials Science and Engineering, Northeastern University, Shenyang 110819, China;
4. Key Laboratory of Dielectric and Electrolyte Functional Material Hebei Province, School of Resources and Materials, Northeastern University at Qinhuangdao, Qinhuangdao 066004, China

Received 25 April 2024; accepted 13 December 2024

Abstract: A clean and efficient process for the direct extraction of valuable metals from low-grade nickel sulfide ore through oxidative leaching with $(NH_4)_2S_2O_8$ under atmosphere pressure was proposed to address the growing demand for nickel and cobalt in the new energy industry. The effects of four key parameters on the metal leaching rates were systematically investigated. Characterization techniques, including XRD, SEM and EDS, were employed to analyze phase transformations during the leaching process. Under optimized conditions, approximately 96.5% of nickel, 95.5% of cobalt and 65.2% of copper were successfully extracted. The kinetics of the leaching process was explored to identify the controlling mechanisms of nickel, cobalt and copper dissolution, establishing activation energies and kinetic equations for each metal. The cleanliness and efficiency of this method were confirmed through comparisons with other extraction processes for nickel sulfide ore.

Key words: nickel sulfide ore; ammonium persulfate; oxidative leaching; phase transformation; leaching kinetics

1 Introduction

In recent years, the rapid development of science and technology has significantly expanded the application of nickel across sectors such as national defense, aerospace, catalysis, and new energy industry. As the primary source of nickel production, high-grade nickel sulfide ores are gradually being depleted, low-grade nickel sulfide ores have become the dominant resource for mining [1,2]. However, the traditional pyrometallurgical processes are unsuitable for low-grade nickel sulfide ores due to their high gangue content [3, 4]. To address this, researchers have explored various hydrometallurgical methods, including atmospheric acid leaching [5,6], high pressure acid leaching [7], ammonia leaching [8], bioleaching [9], and heap leaching [10]. Unfortunately, acid leaching requires large volumes of acid, leading to increased equipment corrosion and maintenance. High-pressure processes demand rigorous equipment specifications, and bioleaching requires prolonged reaction time [11]. Thus, there is an urgent need to develop cleaner, more energy-efficient, and eco-friendly processes for treating nickel sulfide ores.

Corresponding author: Wen-ning MU, Tel: +86-13780335321, E-mail: danae2007@163.com
https://doi.org/10.1016/S1003-6326(25)66942-1

Oxidative leaching is an efficient hydro-metallurgical process. While achieving a high metal recovery, it avoids the release of pollutants such as SO_2 and H_2S from sulfide minerals, thereby eliminating the need for an acid recovery system and reducing equipment costs. Moreover, the use of non-gaseous oxidants enables operation under normal pressure, further lowering costs. Common oxidants used in atmospheric oxidative leaching include H_2O_2, Fe^{3+} salts, HNO_3, O_2, hypochlorite, persulfate, and air [12,13]. For instance, H_2O_2 in HCl system achieved 33% Cu recovery from chalcopyrite [14]. Sodium chlorite, as an oxidant in nitric−sulfuric acid solutions, effectively leached Ni−Cu sulfide tailings, with recoveries of 91.5% Ni, 85.0% Cu and 54.6% Co [15]. Oxidative leaching using Fe^{3+} ions in sulfuric acid recovered 95.61% of tellurium from Dashuigou tellurium ore [16], while a $CuSO_4$−NaCl−H_2SO_4−[Bmim][PF_6] mixture extracted over 92.65% Cu from waste mobile phones [17]. Additionally, ammonium persulfate ($(NH_4)_2S_2O_8$) extracted 81.07% Ni, 93.81% Cu, and 71.74% Co from low nickel matte in an atmospheric ammonia leaching system [18]. Although the metal recovery rates are relatively high, oxidative leaching agents are typically used in combination with other leaching agents, while reports on the use of oxidants alone in sulfide mineral leaching are rare.

Ammonium persulfate, with a standard redox potential of E^{Θ}=2.01 V, exhibits a higher oxidative capacity compared to other common oxidants such as H_2O_2 (E^{Θ}=1.78 V), O_2 (E^{Θ}=0.40 V), $NaClO_3$ (E^{Θ}=1.45 V) and Fe^{3+}/Fe^{2+} (E^{Θ}=0.77 V) [18−21]. Moreover, compared with nitric acid, ammonium persulfate is a safer oxidant. Unlike chloride-containing oxidants, it does not introduce corrosive chloride ions and cause less damage to equipment. These advantages highlight the potential of ammonium persulfate as a standalone oxidant for the oxidative leaching of sulfide minerals. In this work, a novel and efficient process was proposed for extracting valuable metals from low-grade nickel sulfide ore through direct oxidative leaching with $(NH_4)_2S_2O_8$ under atmospheric pressure. The effects of key parameters, including ore particle size, the mass ratio of $(NH_4)_2S_2O_8$ to ore, leaching time and temperature on metal extraction were systematically investigated. Mineral phase transformations and the oxidative leaching mechanism were analyzed using X-ray diffraction (XRD), scanning electron microscope (SEM), and energy disperse spectroscopy (EDS). The cleanliness and efficiency of this process were further validated by comparison with other extraction processes for nickel sulfide minerals.

2 Experimental

2.1 Materials

The low-grade nickel sulfide ore used in this study was provided by the Jinchuan Group, China. The ore was crushed and ground to a particle size range of 90−900 μm for leaching experiments. The chemical composition of the ore was determined by X-ray fluorescence spectrometry (XRF, S8 TIGER II, Germany). As shown in Table 1, the ore contains 3.18% nickel, 1.84% copper and 0.08% cobalt, with impurities such as iron and magnesium present at 21.41% and 8.73%, respectively.

Table 1 Chemical composition of low-grade nickel sulfide ore (wt.%)

Ni	Cu	Co	Mg	Fe	S	O	Si
3.18	1.84	0.08	8.73	21.41	12.05	44.54	8.17

The mineral composition of the ore was analyzed using XRD (Rigaku-Smartlab, Japan), with the results presented in Fig. 1(a). The results indicate that nickel primarily exists as pentlandite ($(Fe,Ni)_9S_8$), copper mainly presents as chalcopyrite ($CuFeS_2$), and magnesium is primarily found in lizardite ($Mg_3Si_2O_5(OH)_4$), talc ($Mg_3Si_4O_{10}(OH)_2$) and magnesium spinel ($MgFe_2O_4$). Iron coexists with nickel, copper and magnesium, and also exists in the form of pyrite (FeS_2), pyrrhotite (Fe_7S_8) and magnetite (Fe_3O_4). The micromorphology and element distribution of the ore were analyzed using a ZEISS-Sigma scanning electron microscope (SEM, Germany) equipped with energy dispersive spectroscopy (EDS). The result presented in Fig. 1(b) reveals that the particles of the ore after crushing and grinding have a blocky structure and irregular particle sizes. As shown in Fig. 1(c), elements such as sulfur, oxygen, iron, copper, magnesium, silicon, cobalt and nickel are uniformly distributed in the ore. All reagents used in the experiments were of analytical grade, and deionized water was used throughout the study.

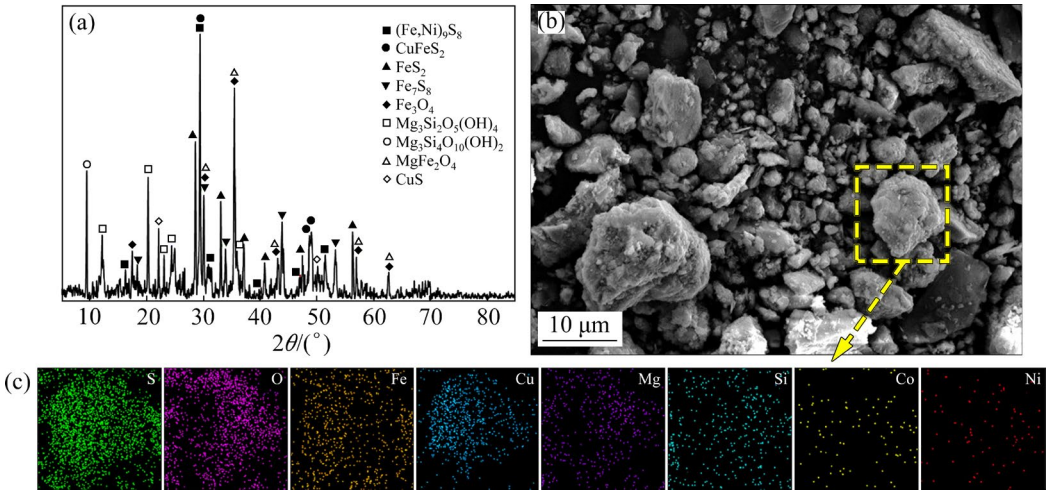

Fig. 1 XRD patterns of low-grade nickel sulfide ore (a), SEM image of nickel sulfide ore (b), and corresponding EDS surface mapping (c)

2.2 Oxidative leaching procedure

The dried ore powder was mixed with $(NH_4)_2S_2O_8$ solution at a liquid-to-solid ratio of 20∶1, and transferred into a three-neck round-bottom flask. Then, the mixture was heated to 50−90 °C in a digital thermostatic water bath with a temperature control accuracy of ±1 °C, and leached for 1−4 h under a predetermined stirring speed. Upon completing the leaching process, the slurry was filtered to separate the leaching solution from the residue. The concentrations of valuable metals in the leaching solution were determined using an atomic absorption spectrophotometer (AAS, AA7000, Shimadzu, Japan), and the metal extractions were calculated using Eq. (1) [22].

$$x_m = \frac{c_m V_m}{w_m m} \times 100\% \quad (1)$$

where x_m stands for the extraction of metal (%), c_m represents the concentration of metal ion in the leaching solution (g/L), V_m denotes the volume of leaching solution (L), m represents the mass of the ore (g), and w_m is the mass fraction of metal elements in the ore (%). Here, m represents metal elements (Ni, Cu, Co, Fe, and Mg).

2.3 Kinetics experiment

A kinetics experiment was conducted to identify the rate-controlling step of the oxidative leaching process. A 5 mL sample was collected every 15 min throughout the entire leaching procedure. To minimize the impact of sampling on the system, an initial leaching solution volume of 1000 mL was used [23]. Each sample was filtered through a funnel to obtain a clear leaching solution, and the metal concentration was subsequently measured using AAS. The metal extraction at various reaction time was calculated using Eq. (1).

3 Results and discussion

3.1 Oxidative leaching process

3.1.1 Effect of ore particle size

Based on our previous study [24], the effect of ore particle size on metal extraction efficiency was investigated under the following conditions: mass ratio of $(NH_4)_2S_2O_8$ to ore of 4.5∶1, liquid-to-solid ratio of 20∶1, leaching time of 4 h, and leaching temperature of 80 °C. As shown in Fig. 2(a), particle size of ore has a significant impact on the extraction of nickel, copper, cobalt and iron. As particle size decreases, the extractions of these metals initially increase, reaching their maximum values respectively at particle sizes of 105−125 μm, and then decrease as the particle size further reduces. The maximum extractions were 96.50% for nickel, 95.50% for cobalt, 65.20% for copper, and 74.30% for iron. The reason why the metal extraction increases with the decrease of particle size is attributed to the large specific surface area, which enhances the interfacial reaction between the leaching agent and the mineral [25]. However, excessively fine particle sizes increase both grinding energy consumption and costs, while also raising the effective viscosity of the leaching solution [26], thereby hindering the diffusion of the

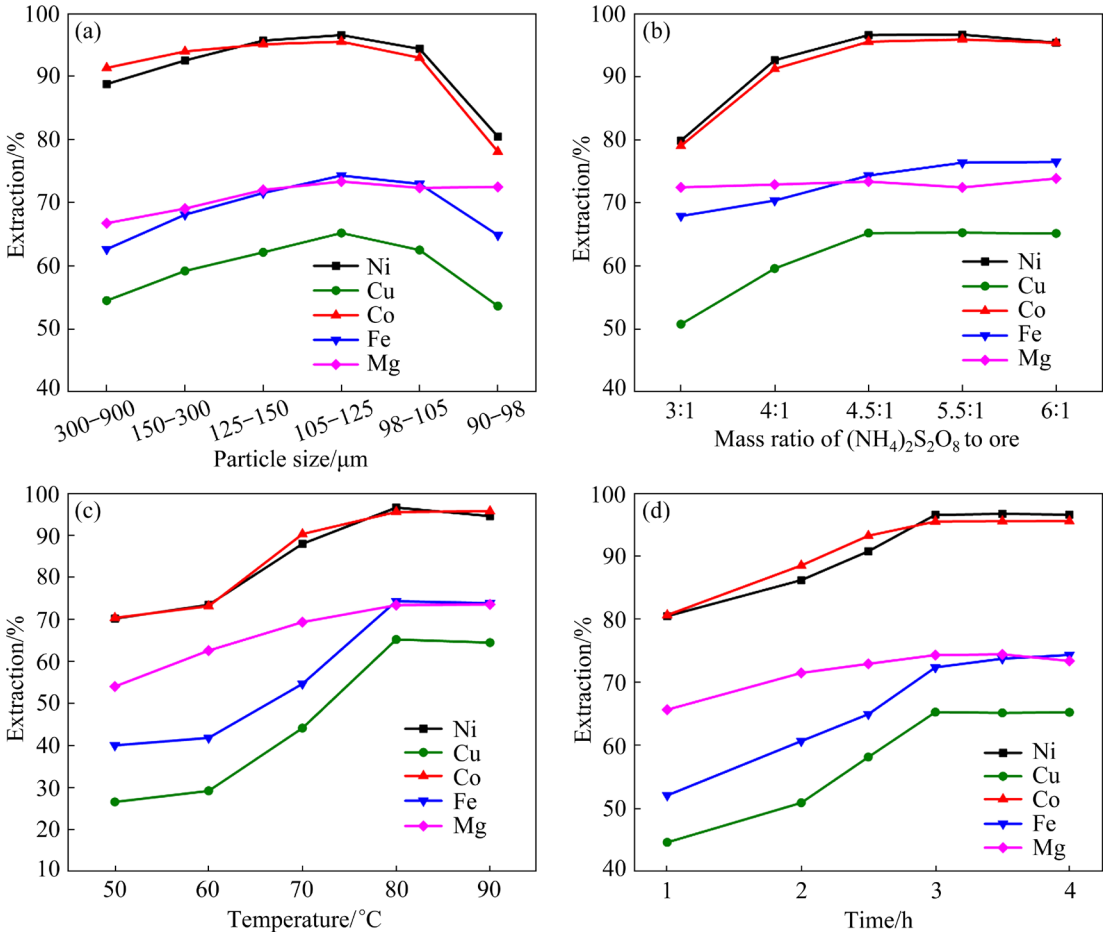

Fig. 2 Effects of leaching parameters on metal extraction: (a) Particle size of ore; (b) Mass ratio of $(NH_4)_2S_2O_8$ to ore; (c) Leaching temperature; (d) Leaching time

leaching agent. In contrast, magnesium extraction is less affected by particle size, fluctuating between 66.7% and 73.3%. To balance grinding energy consumption and metal extraction rates, a particle size range of 300−900 μm is recommended, achieving extractions of 88.79% for nickel, 91.35% for cobalt, 54.51% for copper, 62.65% for iron, and 66.77% for magnesium. However, for maximizing metal extractions, the optimal particle size is chosen as 105−125 μm. These particle size ranges are larger than those reported in previous studies [6,24,27], suggesting that this oxidative leaching process effectively reduces the energy consumption associated with grinding.

3.1.2 Effect of mass ratio of $(NH_4)_2S_2O_8$ to ore

The effect of the mass ratio of $(NH_4)_2S_2O_8$ to ore, ranging from 3∶1 to 6∶1, on metal extraction was investigated, with the results presented in Fig. 2(b). The results indicate that the mass ratio has minimal effect on magnesium extraction but significantly impacts the extraction of nickel, copper, cobalt and iron. As the mass ratio increases from 3∶1 to 4.5∶1, the extractions of nickel, copper, cobalt and iron increase from 79.8%, 50.7%, 79.0% and 67.9% to 96.5%, 65.2%, 95.5% and 74.3%, respectively. However, when the mass ratio exceeds 4.5∶1, its further increase does not lead to significant improvements in metal extractions. This suggests that, the ammonium persulfate dosage is insufficient to fully react with the valuable metals in the ore when the mass ratio is below 4.5∶1. Conversely, when the mass ratio exceeds 4.5∶1, excess ammonium persulfate contributes little to further extraction, leading to inefficient use of the leaching agent. Considering both extraction efficiency and cost, the optimal mass ratio of $(NH_4)_2S_2O_8$ to ore is determined to be 4.5∶1, which achieves high metal recovery without requiring additional acid or ammonia leaching solutions [15,18].

3.1.3 Effect of leaching temperature

As illustrated in Fig. 2(c), the extractions of nickel, cobalt, copper, iron and magnesium exhibit

a similar trend with increasing temperature from 50 to 90 °C, initially rising before reaching a plateau. Notably, between 50 and 60 °C, no significant improvement in metal extraction is observed. However, is can be observed that the extractions of all metals increase significantly and their maximum values are achieved at 80 °C. Beyond this temperature, a slight decrease in extraction is observed, likely due to the hydrolysis of ammonium persulfate. Therefore, 80 °C is selected as the optimal leaching temperature for subsequent experiments.

3.1.4 Effect of leaching time

The effect of leaching time on the completeness of metal reactions was investigated, as shown in Fig. 2(d). As leaching time increases, metal extraction rises initially before stabilizing. Maximum extractions are reached at 3 h, with their extractions of 96.5% for Ni, 95.5% for Co, 65.2% for Cu, 74.3% for Fe, and 73.3% for Mg. This indicates that longer leaching time enhances chemical reactions and improves metal recovery. However, beyond 3 h, further extension of leaching time does not significantly increase extractions, likely due to the completion of the reactions. Therefore, a leaching time of 3 h is recommended for maximizing metal extractions.

3.2 Kinetics of leaching process

3.2.1 Shrinking unreacted core model

The leaching process of low-grade nickel concentrate is a solid−liquid reaction, characterized by the formation of a solid product. This process can be effectively described using the shrinking unreacted core model. In this model, the reaction proceeds through three distinct steps: (1) diffusion of the leaching agent ($(NH_4)_2S_2O_8$) or soluble metal sulfates generated by the reaction across the liquid boundary layer (external diffusion); (2) diffusion of the leaching agent or metal sulfates through the solid sulfur layer formed on the particle surfaces (internal diffusion); (3) interfacial chemical reactions between the leaching agent and the solid particles (interfacial chemical reaction).

The rate equations for the shrinking unreacted core model, controlled by interfacial chemical reaction, internal diffusion, and external diffusion, are expressed as follows: $1-(1-x)^{1/3}=k_r t$, $1-2/3x-(1-x)^{2/3}=k_d t$ and $1-(1-x)^{2/3}=k_b t$ [28,29], where x denotes the extraction of the components, t represents the reaction time, and k_r, k_d and k_b are the apparent rate constants corresponding to each of the control conditions.

According to the Arrhenius equation ($k=A\cdot\exp[-E_a/(RT)]$), the relationship between the apparent rate constant (k) and thermodynamic temperature (T) can be expressed as $\ln k=\ln A-E_a/(RT)$, where A is the frequency factor, E_a denotes the activation energy (J/mol), and R is the molar gas constant. For most leaching process, E_a exceeds 30 kJ/mol when the rate is controlled by interfacial chemical reactions, whereas it is less than 30 kJ/mol when internal diffusion governs the rate [30,31].

3.2.2 Control steps in metal leaching

The relationship between metal extraction (Ni, Cu, Co, Fe and Mg) and time at different temperatures is illustrated in Fig. 3. As shown, the extraction curves for Ni, Co, Mg and Fe exhibit significant changes from 0 to 60 min, followed by a plateau between 75 and 180 min. Consequently, the leaching processes of Ni, Co, Mg and Fe were analyzed in two stages, divided at 60 min, to identify the kinetic control step for each metal. The experimental data presented in Figs. 3(a−d) were analyzed using the three kinetic models previously discussed, with the corresponding linear fitting data provided in Tables S1 and S2 of Supplementary Materials (SM). The results show that the extractions of Ni, Co, Mg and Fe exhibit the highest linear correlation with the interfacial chemical reaction control model during the 0−60 min interval and with the internal diffusion control model during the 75−180 min interval. In contrast, the extraction curve for Cu increases steadily and uniformly over the entire 0−180 min period. Therefore, the three kinetic models were applied to the full dataset for Cu, as illustrated in Fig. 3(e), with the fitting results shown in Table S3 of SM. The results indicate that the extraction of Cu best corresponds to the internal diffusion control model over the 0−180 min period.

Using the $\ln k_r$ and $\ln k_d$ values from Tables S1−S3 of SM, plots of $\ln k_r$ versus $1/T$ and $\ln k_d$ versus $1/T$ are generated, as shown in Fig. 4. The E_a is then calculated using the Arrhenius equation. For the 0−60 min period, the calculated E_a values are 33.64 kJ/mol for Ni, 30.72 kJ/mol for Co, 40.93 kJ/mol for Fe, and 32.13 kJ/mol for Mg,

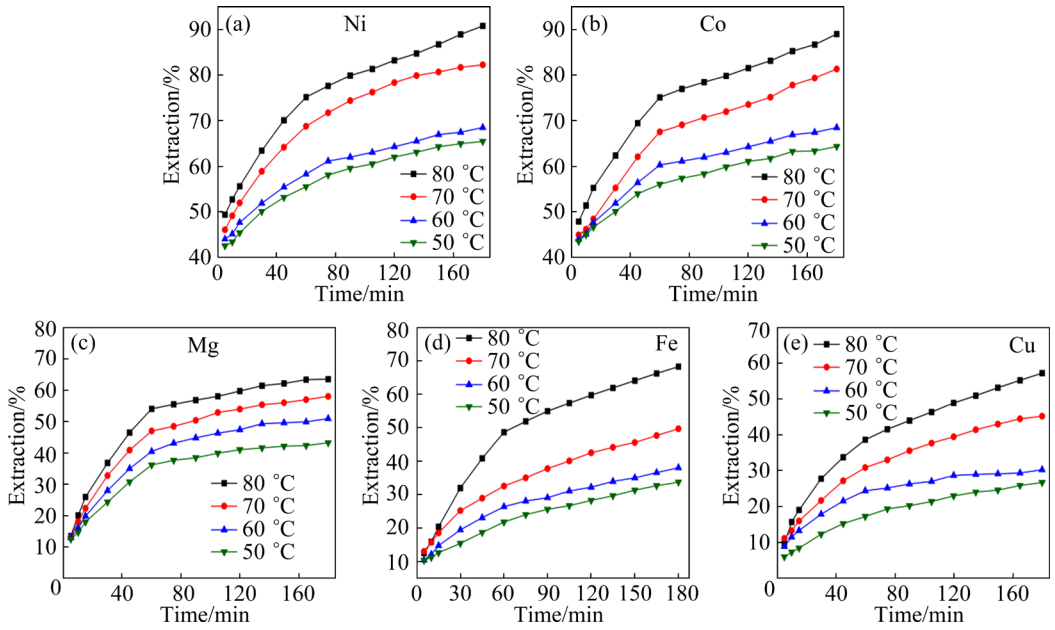

Fig. 3 Relationship between metal extraction and time at various temperatures

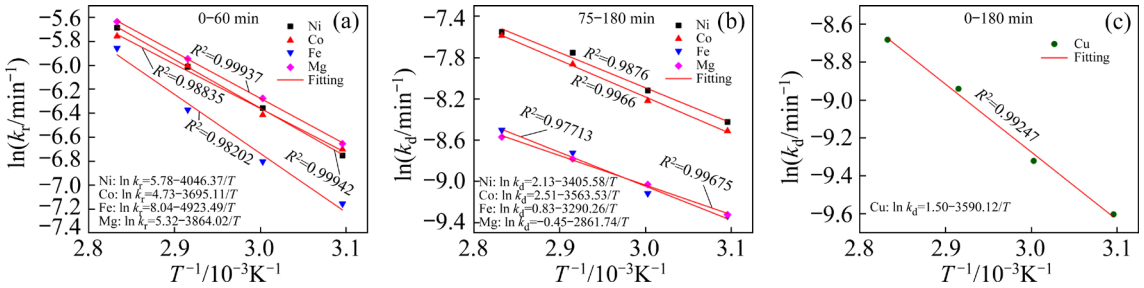

Fig. 4 Relationship between ln k and $1/T$ fitted based on Arrhenius equation at different control stages: (a) Chemical reaction control stage for Ni, Co, Fe and Mg; (b) Diffusion control stage for Ni, Co, Fe and Mg; (c) Diffusion control stage for Cu

indicating that the leaching process for these metals are controlled by interfacial chemical reactions during this time frame. In contrast, the E_a values for Ni, Co, Fe and Mg in the 75−180 min period are 28.31, 29.63, 27.36 and 23.79 kJ/mol, respectively, suggesting that the leaching process during this period are governed by internal diffusion. The E_a value for Cu over the entire 0−180 min period is 29.85 kJ/mol, further confirming that the leaching of Cu is controlled by internal diffusion throughout this time. The rate constants for metal leaching were derived from the intercepts of the fitted lines: 323.76 min^{-1} for Ni, 113.30 min^{-1} for Co, 3102.61 min^{-1} for Fe and 204.38 min^{-1} for Mg during the 0−60 min period; 8.41 min^{-1} for Ni, 12.30 min^{-1} for Co, 2.29 min^{-1} for Fe and 0.64 min^{-1} for Mg during the 75−180 min period; and 4.48 min^{-1} for Cu over the entire 0−180 min period.

The relationship between metal extraction (Ni, Cu, Co, Fe and Mg) and time at various concentrations of $(NH_4)_2S_2O_8$ is illustrated in Fig. 5. The fitting results for the three kinetic control models applied to the experimental data are presented in Tables S4−S6 of SM. As shown in Table S4 of SM, the linear correlation coefficients for the interfacial chemical reaction model exceed 0.99 for Ni, Co, Fe and Mg during the 0−60 min period, indicating a strong fit between this model and the leaching reactions of these metals. Table S5 of SM reveals that the linear correlation coefficients for the internal diffusion model are higher than those for the other two kinetic control models, suggesting that this model best describes the leaching of Ni, Co, Fe and Mg during the 75−180 min period. Table S6 of SM confirms that the leaching of Cu over the 0−180 min period is controlled by internal diffusion.

Using the ln k_r values from Tables S4−S6 of SM, plots of ln k_r versus ln $c_{(NH_4)_2S_2O_8}$ and ln k_d versus ln $c_{(NH_4)_2S_2O_8}$ are generated, as shown in Fig. 6. The slopes of the linear plots, representing the influence index of the initial $(NH_4)_2S_2O_8$ concentration, are determined to be 1.70 for Ni, 2.62 for Co, 2.24 for Fe and 0.49 for Mg within 0−60 min, and 2.19 for Ni, 2.04 for Co, 2.79 for Fe and 1.08 for Mg within 75−180 min. For Cu, the slope is found to be 2.29 over the entire 0−180 min. In summary, the kinetic equations for the leaching of metals are presented in Table 2.

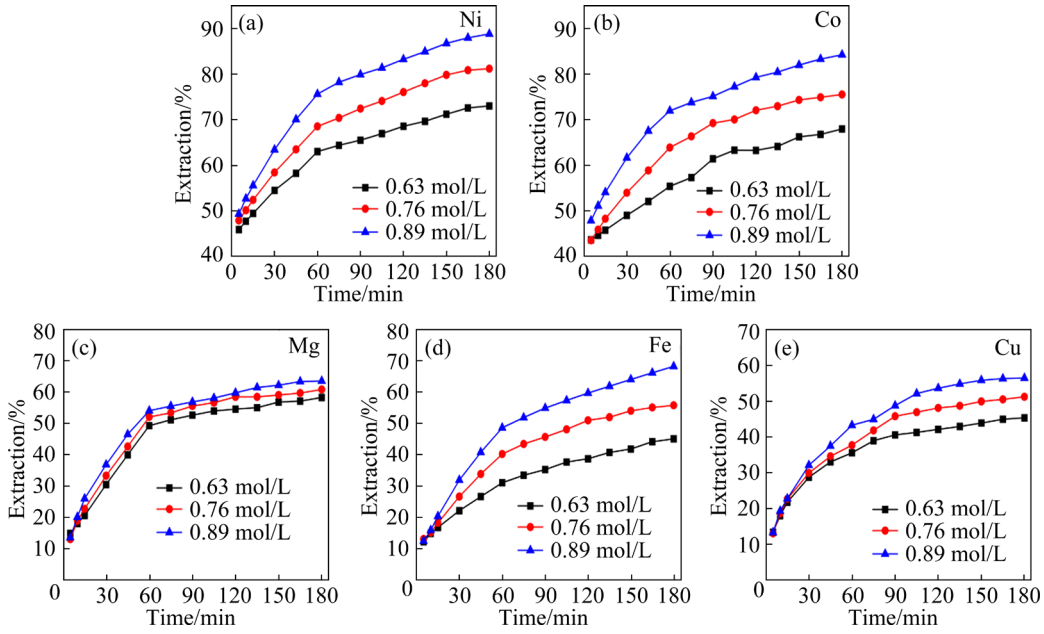

Fig. 5 Relationship between metal extraction and time at different $(NH_4)_2S_2O_8$ concentrations

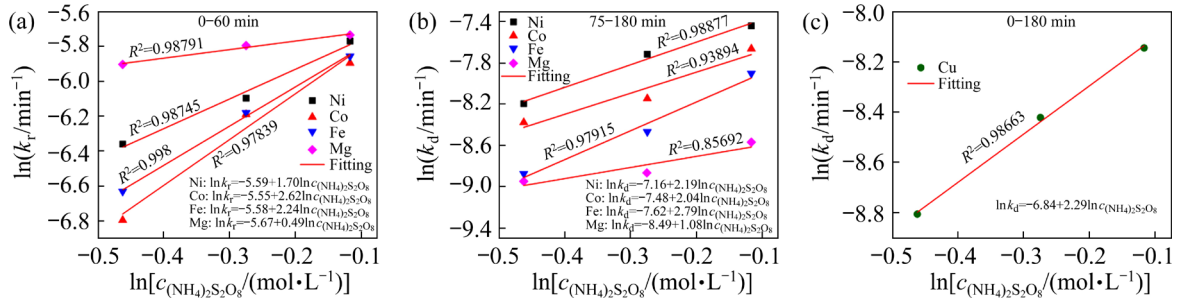

Fig. 6 Relationship between ln k and ln$c_{(NH_4)_2S_2O_8}$ fitted based on Arrhenius equation at different control stages: (a) Chemical reaction control for Ni, Co, Fe and Mg; (b) Diffusion control for Ni, Co, Fe and Mg; (c) Diffusion control for Cu

Table 2 Kinetic equations for metal leaching

Element	0−60 min	75−180 min
Ni	$1-(1-x)^{1/3}=323.76\cdot c_{(NH_4)_2S_2O_8}^{1.70}\exp\left(\frac{33640}{T}\right)t$	$1-2/3x-(1-x)^{2/3}=8.41\cdot c_{(NH_4)_2S_2O_8}^{2.19}\exp\left(\frac{28310}{T}\right)t$
Co	$1-(1-x)^{1/3}=113.30\cdot c_{(NH_4)_2S_2O_8}^{2.62}\exp\left(\frac{30720}{T}\right)t$	$1-2/3x-(1-x)^{2/3}=12.30\cdot c_{(NH_4)_2S_2O_8}^{2.04}\exp\left(\frac{29630}{T}\right)t$
Fe	$1-(1-x)^{1/3}=3102.61\cdot c_{(NH_4)_2S_2O_8}^{2.24}\exp\left(\frac{40930}{T}\right)t$	$1-2/3x-(1-x)^{2/3}=2.29\cdot c_{(NH_4)_2S_2O_8}^{2.79}\exp\left(\frac{27360}{T}\right)t$
Mg	$1-(1-x)^{1/3}=204.38\cdot c_{(NH_4)_2S_2O_8}^{0.49}\exp\left(\frac{32130}{T}\right)t$	$1-2/3x-(1-x)^{2/3}=0.64\cdot c_{(NH_4)_2S_2O_8}^{1.08}\exp\left(\frac{23790}{T}\right)t$
Cu	$1-2/3x-(1-x)^{2/3}=4.48\cdot c_{(NH_4)_2S_2O_8}^{2.29}\exp\left(\frac{29850}{T}\right)t$	

3.3 Mechanism of leaching process

Compared to the XRD pattern of the low-grade nickel sulfide ore in Fig. 1(a), the XRD patterns of the leaching residue in Fig. 7 show the presence of sulfur phases, indicating that sulfur within the sulfide minerals is converted to solid sulfur during oxidative leaching. Additionally, the diffraction peaks corresponding to sulfur at temperatures below 60 °C are weaker than those observed at higher temperatures. This suggests that lower temperatures are less conducive to solid sulfur formation, further confirming that the chemical reaction remains incomplete when the leaching temperature is below 60 °C, leading to fewer reaction products. Moreover, at higher temperatures, the diffraction peaks of nickel sulfide, copper sulfide, magnesium sulfide and iron sulfide are significantly diminished, indicating that elevated temperatures promote the dissolution of metals from the mineral phase into the leaching solution.

The completeness of the oxidative leaching reaction can also be assessed from the SEM images in Fig. 8. The surface corrosion of the mineral after oxidative leaching at 50 °C (Fig. 8(a)) is relatively minor. However, when the leaching temperature is increased to 80 °C, the surface erosion becomes more pronounced, with deeper and larger erosion pits visible in Fig. 8(b), indicating a more complete

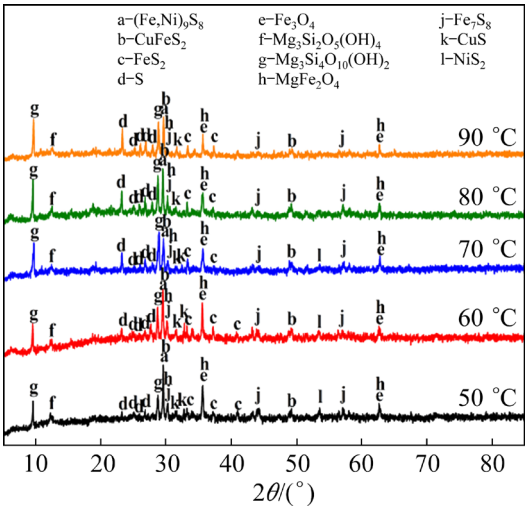

Fig. 7 XRD patterns of leaching residue at different temperatures

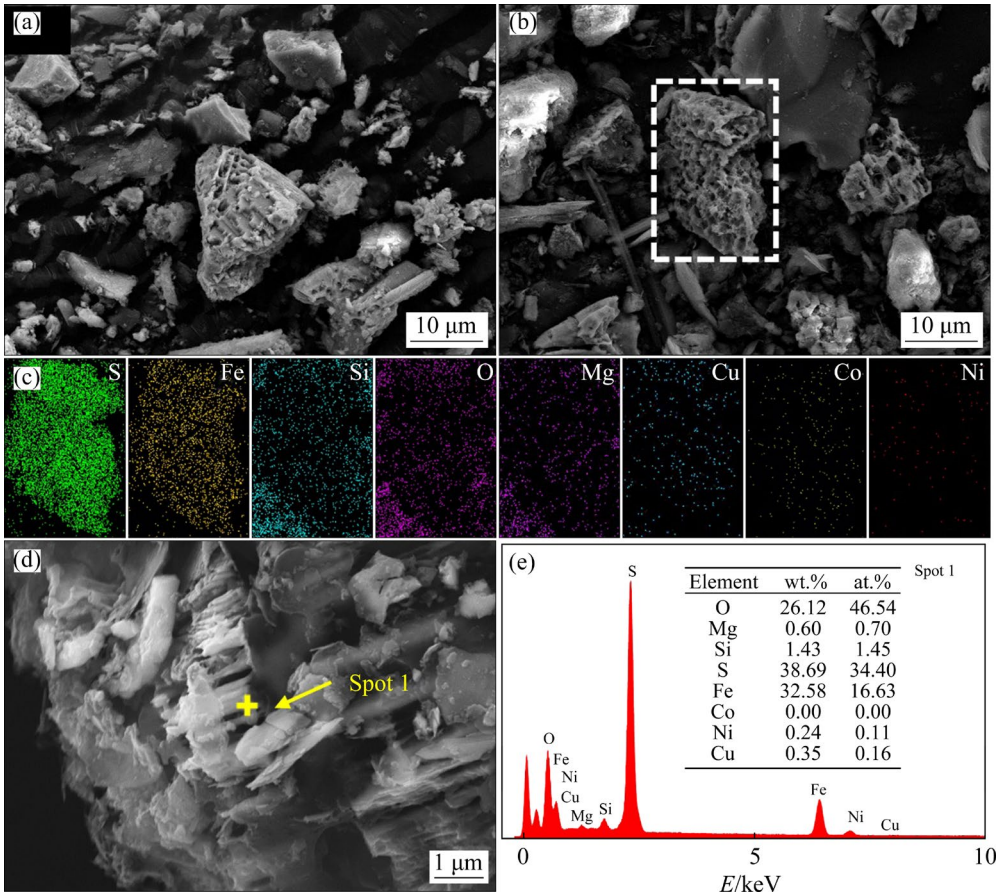

Fig. 8 SEM images of leaching residue at different leaching temperatures: (a) 50 °C; (b) 80 °C; (c) EDS analysis of area in (b); (d) Solid sulfur product layer; (e) EDS analysis of Spot 1

oxidative leaching reaction. Furthermore, the element distribution in Fig. 8(c) reveals that only trace amounts of nickel and cobalt remain in the residue, confirming that nearly all the nickel and cobalt have been converted into metal sulfates and dissolved into the leaching solution. Figure 8(d) shows a distinct product layer on the mineral surface, with a non-uniform distribution resulting from the porous morphology of the leaching residue. Figure 8(e) highlights a substantial sulfur presence at Spot 1, and atomic ratio analysis confirms the presence of free sulfur. Together with the XRD results, this free sulfur is identified as solid sulfur, with an estimated content of approximately 32%.

The chemical reactions involved in the oxidative leaching process are illustrated in Fig. 9. Initially, the sulfide mineral acts as the anode, where sulfur bond to nickel, copper and iron is oxidized to solid sulfur, releasing electrons. Simultaneously, valuable metals such as nickel, copper and iron dissolve into the solution as Ni^{2+}, Cu^{2+} and Fe^{3+} ions, respectively. At the cathode, $S_2O_8^{2-}$ accepts the released electrons and is reduced to SO_4^{2-} [32]. Additionally, some magnesium present in metallic oxides is sulfated by SO_4^{2-}, forming soluble magnesium sulfate. However, due to the continuous formation of solid sulfur and the passivation layer with a unique structure on the surface of chalcopyrite [33], the remaining chalcopyrite becomes tightly encapsulated by insoluble products and a passivation film. As a result, copper extraction is low due to the control of internal diffusion throughout the copper leaching process. To enhance copper extraction, the leaching residue was roasted at 400 °C for 1 h, followed by a secondary leaching with ammonium persulfate, which increases copper extraction from 65.2% to 91.52%.

3.4 Assessment of leaching process

The process parameters for treating nickel sulfide ore in this study are compared with those of other methods, and the results are summarized in Table 3. The findings indicate that this study achieves efficient recovery of nickel and cobalt using a single leaching agent to extract nickel from ore with complex mineral phases. This contrasts with the process that employs ammonium persulfate as an oxidant in a sulfuric acid system to leach low nickel matte [24]. However, the low copper extraction observed here is primarily due to chalcopyrite, the dominant copper-bearing mineral in the ore, being more resistant to leaching compared to bornite. In contrast, the two-stage roasting followed by leaching to recover nickel and copper from low-grade nickel sulfide ore is more complex, and its nickel extraction is lower than that achieved in this study [4]. EKSTEEN et al [34] reported recovering 83.5% Ni and 76.3% Co from a low-grade, serpentine-rich sulfide ore using an alkaline glycine lixiviant system at pH 10 and room temperature. Although the metal recovery is acceptable, the leaching rate is very slow, requiring 672 h. YANG et al [35] proposed a mixed shake flask leaching process for treating low-grade nickel-copper-cobalt sulfide ore at 35 °C, involving acid pre-leaching for 18 d (pH was controlled at 0.8−1.6 with H_2SO_4), followed by bioleaching for 50 d. This process achieved recoveries of approximately 94% nickel, 62% cobalt and 70% copper, but the leaching duration was excessively long.

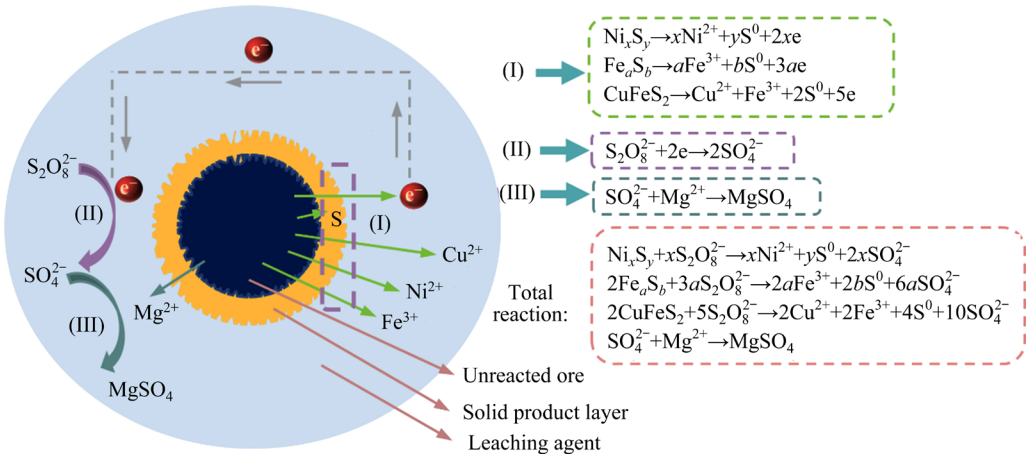

Fig. 9 Leaching reaction mechanism of low-grade nickel sulfide ore

Table 3 Comparison of process parameters and metal extraction efficiency by various nickel sulfide ore processing methods

Process	Condition	Extraction/%				
		Ni	Co	Cu	Fe	Mg
Leaching	$m((NH_4)_2S_2O_8)$:m(ore)=4.5:1, 80 °C, 3 h, particle size 105−125 μm, liquid−solid ratio 20:1 mL/g (This study)	96.5	95.5	65.2	74.3	73.3
Leaching	12.5 g matte, $m((NH_4)_2S_2O_8)$:m(ore)=4.5:1, 80 °C, 4 h, 0.25 mol/L H_2SO_4, particle size 96−106 μm, liquid−solid ratio 20:1 mL/g [24]	91.8	96.6	96.1	66.9	–
Roasting−leaching	Roasting conditions: m(ore):$m(AlCl_3)$=1.5:1, 450 °C, 3 h, particle size 96−80 μm; water leaching conditions: 70 °C, 2 h, liquid−solid ratio 4:1 mL/g [4]	91.6	–	88.5	28.4	16.4
Leaching	m(glycine):m(total metals)=8:1, 672 h, pH 10.0, 40% solids, and room temperature [34]	83.5	76.3	23.7	–	–
Leaching	68 d of flask leaching: 35 °C, 10% w/v pulp density, 180 r/min, 18 d of acid pre-leaching (pH 0.8−1.6 with H_2SO_4 control) and 50 d of bioleaching [35]	94.0	62.0	70.0	–	–

The environmental impact factors of various extraction processes, based on the treatment of 1 kg of nickel sulfide ore, were compared and analyzed, with the results shown in Fig. 10. The findings indicate that the process in this study does not involve the use of acids or alkalis, operates at a lower temperature, and requires a shorter extraction time. As a result, this process exhibits high production efficiency, low energy consumption, and a simplified process flow, in line with low-carbon economy objectives. Furthermore, the sulfur in the nickel sulfide ore remains in the leaching residue as solid sulfur, preventing the emission of SO_2 gas. Waste liquid statistics are based on the volume of leachate used in each process.

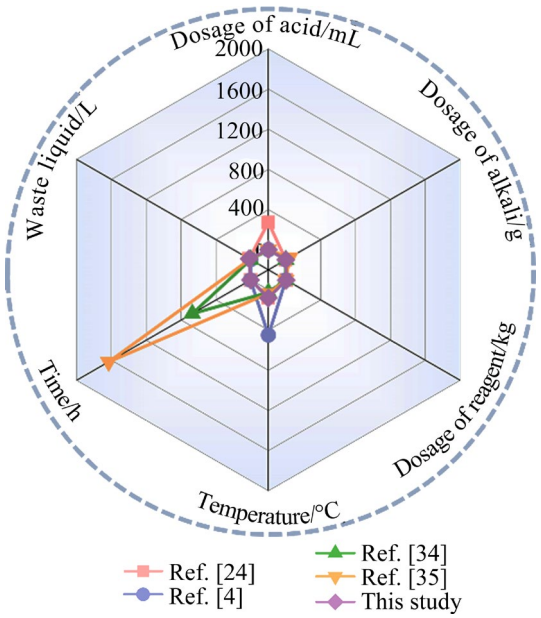

Fig. 10 Schemic of dosage of acid, alkali and reagent, processing temperature, processing time and waste liquid generation for extraction of 1 kg of sulfide minerals

4 Conclusions

(1) A clean and efficient process for extracting valuable metals from low-grade nickel sulfide ore by $(NH_4)_2S_2O_8$ direct oxidative leaching under atmosphere pressure was proposed. The optimal leaching conditions were as follows: particle size of 105−125 μm, mass ratio of $(NH_4)_2S_2O_8$ to ore at 4.5:1, leaching time of 3 h, and leaching temperature of 80 °C. Under these conditions, the extractions for nickel, cobalt, copper, iron and magnesium were 96.5%, 95.5%, 65.2%, 74.3% and 73.3%, respectively.

(2) The leaching kinetics revealed that the leaching of nickel and cobalt was initially controlled by chemical reactions and later by internal diffusion. The entire copper leaching process was governed by internal diffusion. The general kinetic equations for the conversion of Ni and Co can be expressed as $1-(1-x)^{1/3}=A\cdot\exp[-E_a/(RT)]\cdot t$ for the first 0−60 min, and $1-2/3x-(1-x)^{2/3}=A\cdot\exp[-E_a/(RT)]\cdot t$ from 75 to 180 min. For copper conversion, the kinetic equation can be expressed as $1-2/3x-(1-x)^{2/3}=A\cdot\exp[-E_a/(RT)]\cdot t$ over the entire 0−180 min period.

(3) Compared to other metal extraction processes for nickel sulfide ores, this oxidative leaching process was both competitive and eco-friendly. Its advantages include the absence

of acids and alkalis, the elimination of sulfur dioxide and hydrogen sulfide gas emissions, as well as short leaching time and low leaching temperature.

CRediT authorship contribution statement

Rui-min YANG: Methodology, Validation, Data curation, Writing; **Wen-ning MU:** Conceptualization, Methodology, Validation, Writing – Review; **Yuan-hang ZHOU:** Data curation; **Jun-jin MENG:** Data curation; **Xue-fei LEI:** Supervision; **Shao-hua LUO:** Supervision; **Xue-yong DING:** Methodology, Supervision.

Declaration of competing interest

The authors declare that they have no known competing financial interests or personal relationships that could have appeared to influence the work reported in this paper.

Acknowledgments

This work was supported by the National Natural Science Foundation of China (No. 52074069), the Natural Science Foundation of Hebei Province, China (No. E2020501029), the Natural Science Foundation−Steel, the Iron Foundation of Hebei Province, China (No. E2022501030), and Performance Subsidy Fund for Key Laboratory of Dielectric and Electrolyte Functional Material Hebei Province, China (No. 22567627H).

Supplementary Materials

Supplementary Materials in this paper can be found at: https://tnmsc.csu.edu.cn/download/19-p4253-2024-0594-Supplementary_Materials.pdf.

References

[1] MU Wen-ning, CUI Fu-hui, XIN Hai-xia, ZHAI Yu-chun, XU Qian. A novel process for simultaneously extracting Ni and Cu from mixed oxide-sulfide copper-nickel ore with highly alkaline gangue via $FeCl_3·6H_2O$ chlorination and water leaching [J]. Hydrometallurgy, 2020, 191: 105187.

[2] DU Shou-ming, MU Wen-ning, LI Li-ying, SHI Shu-zheng, CHEN Huan-huan, LEI Xue-fei, GUO Rui, LUO Shao-hua, WANG Le. Simultaneous extraction of metals from nickel concentrate via NH_4HSO_4 roasting−water leaching process and transformation of mineral phase [J]. Transactions of Nonferrous Metals Society of China, 2024, 34(3): 1003−1015.

[3] MU Wen-ning, XIAO Teng-fei, SHI Shuang-zhi, XU Xue-qing, CHENG Hao, ZHAI Yu-chun. Co-extraction of valuable metals and kinetics analysis in chlorination process of low-grade nickel-copper sulfide ore [J]. Transactions of Nonferrous Metals Society of China, 2022, 32(6): 2033−2045.

[4] CUI Fu-hui, MU Wen-ning, ZHAI Yu-chun, GUO Xue-yi. The selective chlorination of nickel and copper from low-grade nickel-copper sulfide-oxide ore: Mechanism and kinetics [J]. Separation and Purification Technology, 2020, 239: 116577.

[5] XIAO Wan-hai, LIU Xu-heng, ZHAO Zhong-wei. Kinetics of nickel leaching from low-nickel matte in sulfuric acid solution under atmospheric pressure [J]. Hydrometallurgy, 2020, 194: 105353.

[6] LIU Xu-heng, HUANG Jia-hao, ZHAO Zhong-wei, CHEN Xing-yu, LI Jiang-tao, HE Li-hua, SUN Feng-long. Nickel leaching kinetics of high-grade nickel matte with sulfuric acid under atmospheric pressure [J]. Hydrometallurgy, 2023, 215: 105987.

[7] LI Yun-jiao, PAPANGELAKIS V G, PEREDERIY I. High pressure oxidative acid leaching of nickel smelter slag: Characterization of feed and residue [J]. Hydrometallurgy, 2009, 97(3): 185−193.

[8] MENG X H, HAN K N. The principles and applications of ammonia leaching of metals—A review [J]. Mineral Processing and Extractive Metallurgy Review, 1996, 16(1): 23−61.

[9] SUN Jian-zhi, WEN Jian-kang, CHEN Bo-wei, WU Biao. Mechanism of Mg^{2+} dissolution from olivine and serpentine: Implication for bioleaching of high-magnesium nickel sulfide ore at elevated pH [J]. International Journal of Minerals, Metallurgy, and Materials, 2019, 26(9): 1069−1079.

[10] QIN Wen-qing, ZHEN Shi-jie, YAN Zhong-qiang, CAMPBELL M, WANG Jun, LIU Kai, ZHANG Yan-sheng. Heap bioleaching of a low-grade nickel-bearing sulfide ore containing high levels of magnesium as olivine, chlorite and antigorite [J]. Hydrometallurgy, 2009, 98(1/2): 58−65.

[11] WATLING H R. The bioleaching of nickel-copper sulfides [J]. Hydrometallurgy, 2008, 91(1/2/3/4): 70−88.

[12] WANG Ming-yu, CHEN Bian-fang, HUANG Sheng, YANG Hao-xiang, HU Bin, ZHANG Chang-da, WANG Xue-wen, XU Yun-qing. Extraction of molybdenum and nickel from Ni−Mo ore by acid leaching combined with chlorate oxidation and phosphate complexation [J]. Minerals Engineering, 2018, 124: 63−67.

[13] CHOUBEY P K, LEE J C, KIM M S, KIM H S. Conversion of chalcopyrite to copper oxide in hypochlorite solution for selective leaching of copper in dilute sulfuric acid solution [J]. Hydrometallurgy, 2018, 178: 224−230.

[14] PETROVIĆ S J, BOGDANOVIĆ G D, ANTONIJEVIĆ M M. Leaching of chalcopyrite with hydrogen peroxide in hydrochloric acid solution [J]. Transactions of Nonferrous Metals Society of China, 2018, 28(7): 1444−1455.

[15] XIE Yan-ting, XU Yan-bin, YAN Lan, YANG Ru-dong. Recovery of nickel, copper and cobalt from low-grade Ni−Cu sulfide tailings [J]. Hydrometallurgy, 2005, 80(1/2): 54−58.

[16] SHAO Li-xiong, DIAO Jiang, JI Cheng-qing, LI Gang. A novel and clean process for extracting tellurium and bismuth

from Dashuigou tellurium ore by oxidizing leaching [J]. Hydrometallurgy, 2020, 191: 105205.

[17] HE Jing-feng, YANG Jia-xin, TARIQ S M, DUAN Chen-long, ZHAO Yue-min. Comparative investigation on copper leaching efficiency from waste mobile phones using various types of ionic liquids [J]. Journal of Cleaner Production, 2020, 256: 120368.

[18] CHEN Guang-ju, GAO Jian-ming, ZHANG Mei, GUO Min. Efficient and selective recovery of Ni, Cu, and Co from low-nickel matte via a hydrometallurgical process [J]. International Journal of Minerals, Metallurgy, and Materials, 2017, 24(3): 249−256.

[19] SHI Zhuo-ying, JIN Zhu-ji, XUE Hong-ming, SHI Shuang-ji. Oxidant for chemical mechanical polishing of single crystal diamond [J]. Advanced Materials Research, 2014, 1027: 80−83.

[20] LIU Zhi-xiong, XIANG Yan-hong, YIN Zhou-lan, WU Xian-wen, JIANG Jian-bo, CHEN Yi-guang, XIONG Li-zhi. Oxidative leaching behavior of metalliferous black shale in acidic solution using persulfate as oxidant [J]. Transactions of Nonferrous Metals Society of China, 2016, 26(2): 565−574.

[21] SHAO Bin, HU Gui-hua, ALKEBSI K A, YE Guang-hua, LIN Xiao-qing, DU Wen-li, HU Jun, WANG Mei-hong, LIU Hong-lai, QIAN Feng. Heterojunction-redox catalysts of $Fe_xCo_yMg_{10}CaO$ for high-temperature CO_2 capture and in situ conversion in the context of green manufacturing [J]. Energy & Environmental Science, 2021, 14(4): 2291−2301.

[22] ZHANG Ding-chuan, SUN Feng-long, ZHAO Zhong-wei, LIU Xu-heng, CHEN Xing-yu, LI Jiang-tao, HE Li-hua. Kinetics study on cobalt leaching from cobalt-bearing ternary sulfide in sulfuric acid solution under atmospheric pressure [J]. Transactions of Nonferrous Metals Society of China, 2024, 34(5): 1669−1680.

[23] MU Wen-ning, YANG Rui-min, MENG Jun-jing, LI Meng, LEI Xue-fei, LUO Shao-hua. Eco-friendly and selective separation of nickel and copper from low-grade nickel sulfide ore via sulfur fixation roasting with $MgCO_3$ followed by sulfuric acid leaching [J]. Separation and Purification Technology, 2024, 343: 127094.

[24] MU Wen-ning, ZHONG Peng, GU Meng-fei, SUN Wei-song, XIAO Teng-fei, SHEN Hong-tao, XIN Hai-xia, LEI Xue-fei, LUO Shao-hua, WANG Le. Simultaneous dissolution of nickel, copper and cobalt from low grade nickel matte by $(NH_4)_2S_2O_8$–H_2SO_4 oxidative leaching [J]. Hydrometallurgy, 2023, 221: 106147.

[25] NIE Wen-lin, WEN Shu-ming, FENG Qi-cheng, LIU Dan, ZHOU Yao-wen. Mechanism and kinetics study of sulfuric acid leaching of titanium from titanium-bearing electric furnace slag [J]. Journal of Materials Research and Technology, 2020, 9(2): 1750−1758.

[26] LI M Z, HE Y P, LIU Y D, HUANG C. Effect of interaction of particles with different sizes on particle kinetics in multi-sized slurry transport by pipeline [J]. Powder Technology, 2018, 338: 915−930.

[27] XIAO Wan-hai, LI Yong-li, ZHAO Zhong-wei, LIU Xu-heng. Leaching kinetics of low nickel matte in an aqueous solution of sulfuric acid saturated with $FeSO_4$ and $NiSO_4$ [J]. Separation and Purification Technology, 2021, 276: 119375.

[28] GHARABAGHI M, IRANNAJAD M, AZADMEHR A R. Leaching kinetics of nickel extraction from hazardous waste by sulphuric acid and optimization dissolution conditions [J]. Chemical Engineering Research and Design, 2013, 91(2): 325−331.

[29] AYDOGAN S. Dissolution kinetics of sphalerite with hydrogen peroxide in sulphuric acid medium [J]. Chemical Engineering Journal, 2006, 123(3): 65−70.

[30] BILEN A, BIROL B, SARIDEDE M N, KAPLAN Ş S, SÖNMEZ M Ş. Direct microwave leaching conditions of rare earth elements in fluorescent wastes [J]. Journal of Rare Earths, 2024, 42(6): 1165−1174.

[31] ZHONG Shui-ping. Leaching kinetics of gold bearing pyrite in H_2SO_4–$Fe_2(SO_4)_3$ system [J]. Transactions of Nonferrous Metals Society of China, 2015, 25(10): 3461−3466.

[32] TURAN M D, ALTUNDOĞAN H S. Leaching of a copper flotation concentrate with ammonium persulfate in an autoclave system [J]. International Journal of Minerals, Metallurgy, and Materials, 2014, 21(9): 862−870.

[33] HUA Xiao-ming, ZHENG Yong-fei, XU Qian, LU Xiong-gang, CHENG Hong-wei, ZOU Xing-li, SONG Qiu-shi, NING Zhi-qiang. Interfacial reactions of chalcopyrite in ammonia–ammonium chloride solution [J]. Transactions of Nonferrous Metals Society of China, 2018, 28(3): 556−566.

[34] EKSTEEN J J, ORABY E A, NGUYEN V. Leaching and ion exchange based recovery of nickel and cobalt from a low grade, serpentine-rich sulfide ore using an alkaline glycine lixiviant system [J]. Minerals Engineering, 2020, 145: 106073.

[35] YANG Cong-ren, QIN Wen-qing, LAI Shao-shi, WANG Jun, ZHANG Yan-sheng, JIAO Fen, REN Liu-yi, ZHUANG Tian, CHANG Zi-yong. Bioleaching of a low grade nickel−copper−cobalt sulfide ore [J]. Hydrometallurgy, 2011, 106(1/2): 32−37.

$(NH_4)_2S_2O_8$直接氧化浸出硫化镍矿高效提取有价金属的机理、动力学与过程评价

杨瑞敏[1,2]，牟文宁[1,2,3,4]，周远航[2,3]，蒙俊劲[2,3]，雷雪飞[2,3,4]，罗绍华[2,3,4]，丁学勇[1]

1. 东北大学 冶金学院，沈阳 110819；
2. 东北大学秦皇岛分校 资源与材料学院，秦皇岛 066004；
3. 东北大学 材料科学与工程学院，沈阳 110819；
4. 东北大学秦皇岛分校 资源与材料学院 河北省电介质与电解质功能材料重点实验室，秦皇岛 066004

摘　要：为满足新能源产业对镍和钴日益增长的需求，提出了一种清洁高效的工艺，利用$(NH_4)_2S_2O_8$在常压下直接氧化浸出低品位硫化镍矿，从中提取有价金属。系统研究了 4 个关键因素对金属浸出率的影响。采用 XRD、SEM 和 EDS 等表征技术分析了浸出过程中矿相的演变。在优化条件下，镍、钴和铜的浸出率分别为 96.5%、95.5%和 65.2%。通过动力学研究探索了镍、钴和铜溶解过程中的控制机制，并确定了各金属的活化能和动力学方程。通过与其他硫化镍矿提取工艺的比较，证实了该方法的清洁性和高效性。

关键词：硫化镍矿；过硫酸铵；氧化浸出；矿相转化；浸出动力学

(Edited by Xiang-qun LI)